Generalized Gamma-Laguerre Polynomial Chaos to Model Random Bending of Wearable Antennas

Hendrik Rogier, *Senior Member, IEEE*

***Abstract*—A novel generalized Gamma-Laguerre polynomial chaos expansion is proposed to account for the effect of random variations in lower-bounded design parameters on antenna performance. After fitting a shifted generalized Gamma distribution to data sets of such random variables, a predistorted polynomial chaos expansion is generated based on a set of orthogonal generalized Laguerre polynomials. The new statistical methodology is applied to assess the random change in resonance frequency when bending a wearable antenna around different parts of the human body, such as a leg, an arm and a head. For different data sets, an excellent statistical fit is found to both the estimated probability density function of the bending radius and the resulting statistical distribution of the resonance frequency, while requiring up to 480 times fewer sample evaluations.**

***Index Terms*—Microstrip antennas, Random variables, Statistical analysis, flexible electronics, textile antennas**

I. Introduction

Current-generation antenna systems suffer from significant variability, due to fabrication tolerances, and uncertainty, due to variable and adverse deployment conditions [1]–[4]. Important random changes in geometry and material properties are encountered both in high-end applications [5], due to operating frequencies beyond 6 GHz and corresponding small features, and in Internet-of-Things systems [6], given the cheap fabrication techniques and harsh operating environments.

Frequently, random variations in design parameters such as amplitude, permittivity and bending radius, are lower-bounded because of mathematical, physical or practical reasons. Statistical variations induced by such variables are often inaccurately modeled by distributions in the Wiener-Askey generalized polynomial chaos (gPoC) [7]. The generation of a custom set of orthogonal polynomials for a dedicated gPoC expansion requires time-consuming and ill-conditioned Gram–Schmidt [8] or Modified Chebyshev [9]–[11] algorithms.

This letter fits a shifted generalized Gamma distribution [12]–[14] to such design parameters. After predistorting the random variable, a gPoC expansion is constructed based on a set of orthogonal generalized Laguerre polynomials [15, p. 892]. The new scheme is applied to assess the random change in resonance frequency when bending a wearable antenna [16]–[21] around different parts of the human body. The statistical variations in bending radius due to different body morphologies are described by fitting shifted generalized Gamma distributions to different data sets and then processing them through a well-established cylindrical bending model for textile antennas [22]. An excellent statistical fit is obtained for both the estimated probability density function (PDF) of the bending radius and for the resulting statistical distribution of the resonance frequency, compared to a, much slower, Monte Carlo procedure and to existing gPoC procedures. Even for a bimodal distribution of the bending radius, when considering a population consisting of both adults and children, an outstanding fit is found based on a mixture of generalized Gamma distributions, applied as input random variables.

As an alternative to time-consuming Monte-Carlo analysis, several efficient statistical methods were recently proposed to account for variability and uncertainty in electronic circuit and antenna design, focussing on improving the gPoC expansion's effectiveness for a large number of normally [23]–[28] or uniformly [23], [29]–[31] distributed random variables. Moreover, dedicated sets of orthogonal polynomials were generated to improve the gPoC's efficiency [10], [11] or to truncate the Gaussian distribution [9], [32]. Yet, less attention was paid to achieving a better fit between the measured variations' histogram and the gPoC's input random variables' distribution.

Section II outlines the non-intrusive generalized Gamma-Laguerre polynomial chaos, applied in Section III to assess resonance frequency shifts due to cylindrical bending of textile antennas. Section IV studies wearable antenna deployment on different body parts of a representative subset of the military and civilian population. The variations in measured body morphologies, according to these data sets, are first fitted to an Amoroso distribution, which is then transformed in the bent antenna's resonance frequency's distribution.

II. Theory

The lower-bounded, four-parameter, shifted generalized Gamma distribution [12], also denoted Amoroso [13], [14] and Stacy-Mihram distribution, encompasses as special cases more than 50 distinct distributions. Therefore, consider a real, lower bounded, design parameter X, randomly varying according to this distribution with PDF

$$\begin{aligned}\mathcal{P}^X(x) &= \frac{|\gamma|}{\beta\Gamma(\alpha)}\left(\frac{x-\mu}{\beta}\right)^{\alpha\gamma-1} e^{-\left(\frac{x-\mu}{\beta}\right)^{\gamma}}, \quad x>\mu,\\ &= 0, \qquad\qquad\qquad\qquad\qquad\quad x\leq\mu, \quad (1)\end{aligned}$$

with $\alpha > 0$ and γ real shape parameters, β a positive real scale parameter, and μ a real location parameter as the distribution's lower bound. Given a sample set, these parameters are estimated [33], [34] by either maximizing the log-likelihood function [35, p. 227] [36], matching the

H. Rogier is with the Electromagnetics Group, Department of Information Technology, Ghent University-imec, 9052 Ghent, Belgium (e-mail: hendrik.rogier@ugent.be).

cumulants, the raw, central or factorial moments [37, pp 2092–2098]. First, transform the design parameter X, according to [35, p. 69, Section 2.4.2], to a new random variable

$$Y = \left(\frac{X-\mu}{\beta}\right)^{\gamma}, \tag{2}$$

now distributed according to the standard Gamma distribution

$$\begin{aligned}\mathcal{P}^Y(y) &= \frac{1}{\Gamma(\alpha)} y^{\alpha-1} e^{-y}, && y > 0,\\ &= 0, && y \leq 0.\end{aligned} \tag{3}$$

Its gPoC expansion leverages the orthonormal set of generalized Laguerre polynomials [15, p. 892]

$$L_n^{\alpha-1}(y) = \sqrt{\frac{n!}{\Gamma(n+\alpha)}} \sum_{i=0}^{n} (-1)^i \binom{n+\alpha-1}{n-i} \frac{x^i}{i!}, \tag{4}$$

which are orthogonal with respect to (3). Hence, to determine the statistics of an antenna figure of merit's random parameter Z, approximate $Z = F(Y) = F\left[\left(\frac{X-\mu}{\beta}\right)^{\gamma}\right] = f(X)$ by the predistorted polynomial expansion [7] of order P

$$Z(X) \approx F^P(Y(X)) = \sum_{n=0}^{P} z_n^X L_n^{\alpha-1}\left[\left(\frac{X-\mu}{\beta}\right)^{\gamma}\right], \tag{5}$$

converging exponentially according to the Cameron-Martin theorem for $P \to \infty$. To determine the unknown expansion coefficients z_n^X, apply spectral projection, yielding

$$z_n^X = E[Z(y) L_n^{\alpha-1}(y)] = \int_{y=0}^{+\infty} F(y) L_n^{\alpha-1}(y) d\mathcal{P}^Y(y) \tag{6}$$

$$= \int_{x=\mu}^{+\infty} f(x) L_n^{\alpha-1}\left[\left(\frac{x-\mu}{\beta}\right)^{\gamma}\right] d\mathcal{P}^X(x). \tag{7}$$

Now approximate the integral in (6) by the N-point Gauss-generalized-Laguerre quadrature rule

$$z_n^X \approx \sum_{i=1}^{N} w_i F(y_i) L_n^{\alpha-1}(y_i), \qquad n = 0, 1, \ldots, P; \tag{8}$$

its quadrature points y_i being the N zeros of $L_N^{\alpha-1}(y)$ in $[0, +\infty]$, determined by the Golub-Welsch [38] algorithm via the recursion relation of the generalized Laguerre polynomials, with w_i the corresponding weights. Note that one can directly discretize (7) by the N-point quadrature rule

$$z_n^X \approx \sum_{i=1}^{N} w_i f(x_i) L_n^{\alpha-1}\left[\left(\frac{x_i-\mu}{\beta}\right)^{\gamma}\right], n = 0, 1, \ldots, P; \tag{9}$$

with $x_i = \mu + \beta y_i^{\frac{1}{\gamma}}$ the quadrature points in the random design variable X. Hence, the z_n^X are found after evaluating $Z = f(X)$ for N realizations of the random variable X at the quadrature points x_i. The moments of the output distribution $\mathcal{P}^Z$ are computed as

$$\begin{aligned}E[g(z)] &= \int_{\Omega_Z} g(z) d\mathcal{P}^Z(z)\\ &= \int_{x=\mu}^{\infty} g(f(x)) d\mathcal{P}^X(x) \approx \sum_{i=1}^{N} w_i g\left[f(x_i)\right],\end{aligned} \tag{10}$$

for an arbitrary function $g(z)$.

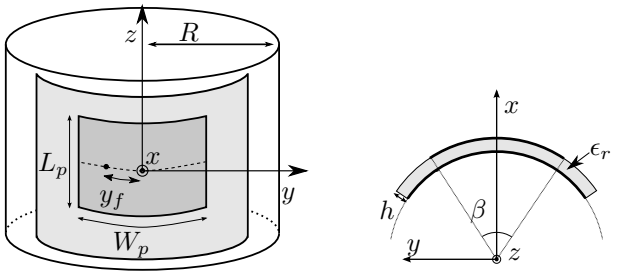

Fig. 1. Wearable antenna subject to cylindrical bending: top (left) and side (right) views.

III. Application: Cylindrical Bending of Wearable Antennas

To showcase the new approach, we apply the method to evaluate cylindrical bending of wearable antennas following the model of [22], comparing to results previously obtained in [9]. For a flexible rectangular patch antenna of length L_p and width W_p, on a textile substrate of thickness h and permittivity ϵ_r, the shift in resonance frequency due to cylindrical bending in the direction of the patch width W_p with curvature radius R (Fig. 1) is found by solving

$$J'_{k_\phi}(k_\rho R) Y'_{k_\phi}\left(k_\rho(R+h)\right) = J'_{k_\phi}\left(k_\rho(R+h)\right) Y'_{k_\phi}(k_\rho R), \tag{11}$$

with $k_\phi = \frac{m\pi}{\beta}$, $k_z = \frac{n\pi}{L_p}$, and $k_\rho = \sqrt{k^2 - k_z^2}$. The angle β is derived from $W = \beta(R + hd)$, with $d = 0.5$ for perfectly stretchable patches and $d = 1$ for completely non-stretchable patches. Substrate compression is accounted for by setting $\epsilon_{r,\text{comp}} = \epsilon_{r,\text{flat}}\left(1 + \eta \frac{h[mm](d-0.5)}{R[m]}\right)$, with η a substrate-dependent empirical parameter, determined by measurements. For non-magnetic substrates, the resonance frequency f_r of the bent patch follows from $k = 2\pi f_r \sqrt{\mu_0 \epsilon_0 \epsilon_{r,\text{comp}}}$. Alternatively, the antenna may be bent along L_p, but, for conciseness, we only discuss bending along the width W_p, which gives rise to the largest variation in resonance frequency.

IV. Results

TABLE I
Parameters of the shifted generalized Gamma distributions fitted to different data sets. Cramér-von Mises test statistic $T = N_{\text{samples}}\omega^2$ as a measure for the distance between CDFs of the data set and the fitted distribution.

Data set	NHANES 2011 Arm radius		ANSUR-II 2012 Head radius		Heinz Thigh radius
	Child	Adult	Female	Male	Adult
N_{samples}	2476	7223	1986	4082	507
α	75.61	8.35	13.98	29.87	52.24
β	32.2 km	5.21 mm	2.00 mm	4.18 mm	16.0 μm
γ	-0.293	1.215	1.304	1.859	0.533
μ	1.51 cm	2.19 cm	7.43 cm	6.55 cm	6.33 cm
T	0.191	0.324	0.298	0.202	0.0419

We now validate the new gPoC framework by considering bending of textile antenna prototypes 2 and 4, previously investigated in [9]. Prototype 2 ($L_\text{p} = 81.2$ mm, $W_\text{p} = 69.25$ mm, $y_f = 16$ mm, $h = 2$ mm, $\epsilon_r = 1.75$, $\eta = 1589$

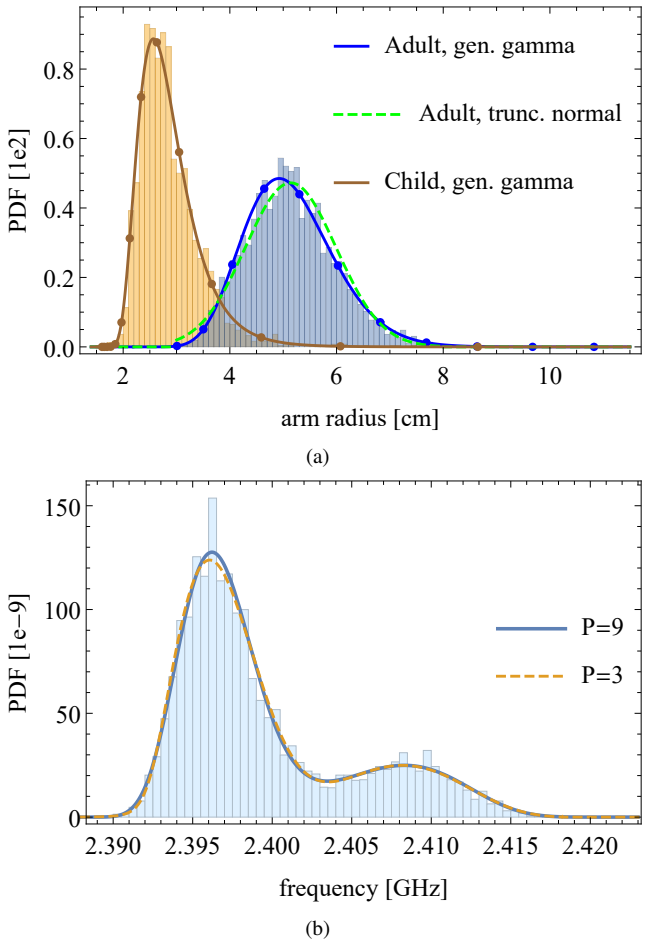

Fig. 2. Prototype 4 textile 2.45GHz antenna on the arm of a representative part of the American population: (a) Histogram and fitted PDF of arm radius of children (brown) and adults (blue) in the NHANES 2011 data set. (b) Histogram of antenna resonance frequency for the complete data set and PDF obtained as a mixture of PDFs for children and adults generated by the Gamma-Laguerre gPoC model.

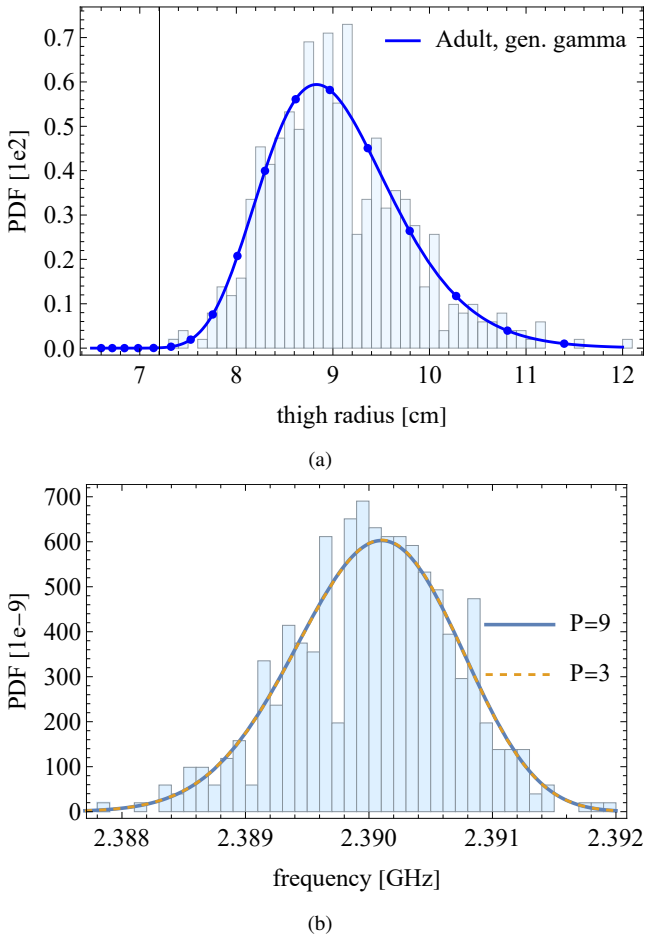

Fig. 3. Prototype 4 textile 2.45GHz antenna on the thigh of 247 men and 260 women, primarily in their twenties and thirties: (a) Histogram and fitted PDF of thigh radius (blue). (b) Histogram of antenna resonance frequency for the Heinz data set and PDF generated by Gamma-Laguerre gPoC model, orders 3 (Cramér-von Mises statistic $T = 0.0404$) and 9 ($T = 0.0419$).

and $d = 1$), implemented in non-stretchable copper foil on an aramid fabric substrate, exhibits a sharp resonance peak close to the 1.57 GHz GPS band. Prototype 4 ($L_\mathrm{p} = 52.5$ mm, $W_\mathrm{p} = 43.7$ mm, $y_f = 11$ mm, $h = 2.7$ mm, $\epsilon_r = 1.715$, $\eta = 1472$ and $d = 1$), fabricated in copper foil on a cotton substrate, resonates in the vicinity of the 2.45 GHz ISM band. Let us first deploy prototype 2 on the head of a soldier and consider the distribution of the head radius of female and male military personnel from the ANSUR-II 2012 data set [39]. Next, let us bend prototype 4 around the arm of a member of the general population, according to the distribution of the arm radius of children (persons smaller than 1.40 m or lighter than 40 kg) and adults listed in the NHANES 2011 database [40]. Finally, let us bend prototype 4 along the thigh of a population of 247 men and 260 women in their twenties and thirties, with their thigh girths listed in the Heinz data set [41].

In a first step, we fit shifted generalized Gamma distributions to the different data sets. The parameters of the PDF (1) of the curvature radius R, found by maximizing the log-likelihood function, are listed in Table I. To verify the goodness of fit, also the Cramér-von Mises test statistic [42] $T = N_\mathrm{samples}\omega^2$ is provided as a measure for the distance ω^2 between the CDFs of the data sets and the fitted distributions, with N_samples the number of samples in each data set. Compared to fitting a truncated Gaussian distribution, as in [9], which yields $T = 2.68$ when applied to the NHANES data set of adults (defined as persons taller than 1.40 m and heavier than 40 kg), excellent fits are obtained here for all data sets, as is confirmed by visual inspection of the histograms and fitted PDFs in Figs. 2(a), 3(a) and 4(a). Moreover, remark that an inverted generalized Gamma distribution ($\gamma < 0$) was obtained for the children's NHANES data set, which can only be approximated very poorly ($T = 8.82$) by a truncated Gaussian distribution.

In a second step, the framework described in Section II is applied to determine the distribution of the resonance frequency, when the antenna prototypes are subject to bending, following the model outlined in Section III. A polynomial model of order $P = 9$ is constructed, based on $N = 15$ quadrature points y_i corresponding to the zeros of $L_N^{\alpha-1}(y)$, shown by the markers in Figs. 2(a), 3(a) and 4(a). Figs. 2(b), 3(b), and 4(b) demonstrate that the resulting PDFs of the resonance frequency correspond very well to the histograms

TABLE II
MOMENTS OF THE RESONANCE FREQUENCY DISTRIBUTION DERIVED FROM THE DATA SET AND THE GPOC EXPANSIONS. CRAMÉR-VON MISES TEST STATISTIC $T = N_{\text{SAMPLES}}\omega^2$ AS A MEASURE FOR THE DISTANCE BETWEEN(*) CDFS OF ARM RADIUS DERIVED FROM THE ORIGINAL DATA SET AND FITTED GENERALIZED GAMMA DISTRIBUTION, AND BETWEEN CDFS OF THE RESONANCE FREQUENCY DISTRIBUTION DERIVED FROM THE DATA SET AND FROM THE GPOC EXPANSIONS.

	NHANES 2011, Arm radius, child			NHANES 2011, Arm radius, adult		
Moment/ distance	data set $N_{\text{samples}} = 2476$	Gamma/Laguerre $P = 9,\ N = 15$	truncated Gaussian $P = 9,\ N = 15$	data set $N_{\text{samples}} = 7223$	Gamma/Laguerre $P = 9,\ N = 15$	truncated Gaussian $P = 9,\ N = 15$
mean [GHz]	2.40752	2.40752 $(-2.6 \times 10^{-5}\%)$	2.40752 $(+3.3 \times 10^{-5}\%)$	2.39665	2.39665 $(+5.6 \times 10^{-6}\%)$	2.39663 $(-7.6 \times 10^{-4}\%)$
std. dev. [MHz]	3.95748	4.02476(+1.6%)	4.68337(+18%)	2.34748	2.34636(−0.05%)	2.44419(+4.1%)
skewness	-0.301144	-0.31969(−6.2%)	0.788587(+362%)	0.360644	0.34680(−3.8%)	0.744016(+106%)
kurtosis	3.26279	2.92163(−10%)	3.60091(+10%)	3.04788	3.06015(+0.4%)	3.562234(+17%)
T	0.19128*	0.19129	8.81993	0.32431*	0.32993	2.67825

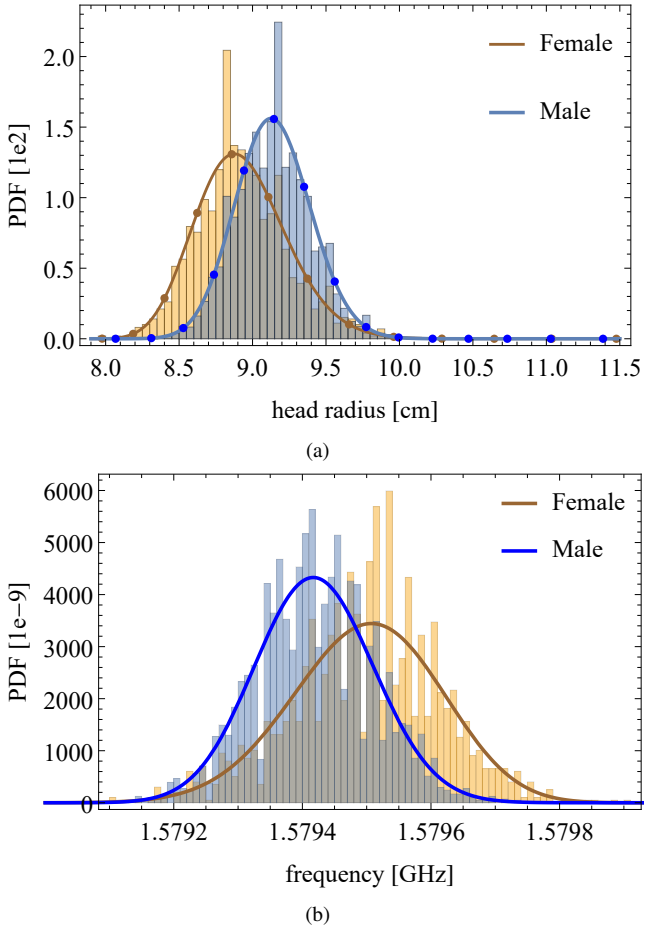

Fig. 4. Prototype 2 textile GPS antenna on the head of a representative part of the American military: (a) Histogram and fitted PDF of head radius of female (brown) and male (blue) personnel in the ANSUR-II 2012 data set. (b) Histograms of antenna resonance frequency and PDFs obtained for female (Cramér-von Mises statistic $T = 0.321$ for order 3 and $T = 0.298$ for order 9) and male soldiers (Cramér-von Mises statistic $T = 0.203$ for order 3 and $T = 0.202$ for order 9), curves shown for order 3.

obtained by processing all data samples using the model in Section III, while requiring significantly fewer solutions of (11), being N versus N_{samples}. The accuracy of the technique is also confirmed by the Cramér-von Mises test statistic T of the output distribution, whose value remains in the same order of magnitude for the output distribution (compared to the data sets' histograms of the resonance frequency) as for the input distribution (compared to the data sets' histograms of the curvature radius), as seen in the last row of Table II and in the captions of Figs. 3 and 4. Table II further shows that (10) accurately computes all relevant lowest-order moments of the resonance frequency distributions. In contrast, for the NHANES data set, observe that the use of a truncated Gaussian distribution, as in [9], yields much less accurate approximations for the corresponding histogram, given the high T-values and deviations in the calculated lowest-order moments. In contrast, with the new method a gPoC approximation of degree $P = 3$ already provides very accurate results, as seen in Figs. 2(b) and 3(b), and demonstrated by the T-values of such an approximation, being only slightly higher than those for $P = 9$, proving the quick convergence of the technique. A final test artificially implements more severe detuning by bending prototype 4 along the arm. Therefore, the effect of compression on substrate permittivity is increased by setting $\eta = 14720$, which is a factor 10 larger than measured [22]. For the NHANES adults data set, the PDF of the Gamma-Laguerre gPoC model of order $P = 3$ ($T = 0.46656$) yields a good fit to the histogram of the antenna resonance frequency, and the PDF of order $P = 9$ ($T = 0.32802$) an excellent fit. For the NHANES children data set, the Gamma-Laguerre gPoC model's PDFs of both orders $P = 3$ ($T = 0.20506$) and $P = 9$ ($T = 0.19123$) provide an excellent fit to the histogram of the antenna resonance frequency.

V. CONCLUSION

Fitting lower-bounded random design variables to an Amoroso distribution and leveraging generalized Laguerre polynomials in a subsequent polynomial chaos expansion yields a highly accurate and efficient statistical design tool, whose input and output PDFs differ only by a small Cramér-von Mises distance from the histograms of the complete data sets while requiring up to 480 times fewer computationally intensive simulations for the examples considered in this letter. The method may be easily extended to other applications subject to lower or upper bounded ($\beta < 0$) random variations. Moreover, the technique may also be applied to multiple statistically independent Amoroso-distributed random variables. Yet, special care is needed when correlations exist between these random inputs. Further research is required to extend the method to multivariate Gamma [43] and Amoroso distributions [44], [45].

REFERENCES

[1] A. Pietrenko-Dabrowska, S. Koziel, and M. Al-Hasan, "Expedited yield optimization of narrow- and multi-band antennas using performance-driven surrogates," *IEEE Access*, vol. 8, pp. 143 104–143 113, 2020.

[2] L. Leifsson, X. Du, and S. Koziel, "Efficient yield estimation of multiband patch antennas by polynomial chaos-based kriging," *Int. J. Numer. Model.-Electron. Netw. Device Fields*, vol. 33, no. 6, p. e2722, 2020.

[3] I. Syrytsin, S. Zhang, G. F. Pedersen, K. Zhao, T. Bolin, and Z. Ying, "Statistical investigation of the user effects on mobile terminal antennas for 5G applications," *IEEE Trans. Antennas Propag.*, vol. 65, no. 12, pp. 6596–6605, 2017.

[4] A. Sibille, "Statistical modeling of the radio-electric properties of wireless terminals in their environment," *IEEE Antennas and Propag. Mag.*, vol. 54, no. 6, pp. 117–129, 2012.

[5] S. Kumar, A. S. Dixit, R. R. Malekar, H. D. Raut, and L. K. Shevada, "Fifth generation antennas: A comprehensive review of design and performance enhancement techniques," *IEEE Access*, vol. 8, pp. 163 568–163 593, 2020.

[6] N. F. M. Aun, P. J. Soh, A. A. Al-Hadi, M. F. Jamlos, G. A. Vandenbosch, and D. Schreurs, "Revolutionizing wearables for 5G: 5G technologies: Recent developments and future perspectives for wearable devices and antennas," *IEEE Microw. Mag.*, vol. 18, no. 3, pp. 108–124, 2017.

[7] D. Xiu and G. E. Karniadakis, "The Wiener-Askey polynomial chaos for stochastic differential equations," *SIAM J. Sci. Comput*, vol. 24, no. 2, pp. 619–644, 2002.

[8] C. Cui and Z. Zhang, "Stochastic collocation with non-gaussian correlated process variations: Theory, algorithms, and applications," *IEEE Trans. Comp., Hybr., Manufac. Techn.*, vol. 9, no. 7, pp. 1362–1375, 2019.

[9] F. Boeykens, H. Rogier, and L. Vallozzi, "An Efficient Technique Based on Polynomial Chaos to Model the Uncertainty in the Resonance Frequency of Textile Antennas Due to Bending," *IEEE Trans. Antennas Propag.*, vol. 62, no. 3, pp. 1253–1260, Mar. 2014.

[10] Z. Zhang, X. Yang, I. V. Oseledets, G. E. Karniadakis, and L. Daniel, "Enabling high-dimensional hierarchical uncertainty quantification by ANOVA and tensor-train decomposition," *IEEE Trans. on CAD of Integrated Circuits and Systems*, vol. 34, no. 1, pp. 63–76, 2015.

[11] Z. Zhang, K. Batselier, H. Liu, L. Daniel, and N. Wong, "Tensor computation: A new framework for high-dimensional problems in EDA," *IEEE Trans. on CAD of Integrated Circuits and Systems*, vol. 36, no. 4, pp. 521–536, 2017.

[12] E. W. Stacy, "A generalization of the gamma distribution," *Ann. Math. Statist.*, vol. 33, no. 3, pp. 1187–1192, Sep. 1962.

[13] G. E. Crooks, "The Amoroso distribution," *arXiv*, no. 1005.3274, 2015. [Online]. Available: https://arxiv.org/abs/1005.3274v2

[14] M. King, *Amoroso Distribution*. John Wiley & Sons, Ltd, 2017, ch. 34, pp. 525–528. [Online]. Available: https://onlinelibrary.wiley.com/doi/abs/10.1002/9781119383536.ch34

[15] G. B. Arfken, H. J. Weber, and F. E. Harris, "Chapter 18 - more special functions," in *Mathematical Methods for Physicists*, 7th ed., G. B. Arfken, H. J. Weber, and F. E. Harris, Eds. Boston: Academic Press, 2013, pp. 871–933.

[16] L. Corchia, G. Monti, and L. Tarricone, "Wearable antennas: Nontextile versus fully textile solutions," *IEEE Antennas and Propag. Mag.*, vol. 61, no. 2, pp. 71–83, 2019.

[17] A. Tronquo, H. Rogier, C. Hertleer, and L. Van Langenhove, "Robust planar textile antenna for wireless body LANs operating in 2.45 GHz ISM band," *IEE Electronic Letters*, vol. 42, no. 3, pp. 142–146, 2006.

[18] I. Locher, M. Klemm, T. Kirstein, and G. Troster, "Design and characterization of purely textile patch antennas," *IEEE Trans. Adv. Packag.*, vol. 29, no. 4, pp. 777–788, December 2006.

[19] P. Salonen and Y. Rahmat-Samii, "Textile antennas: Effects of antenna bending on input matching and impedance bandwidth," *IEEE Trans. Aerospace Electron. Systems*, vol. 22, no. 12, pp. 18–22, December 2007.

[20] C. Hertleer, H. Rogier, L. Vallozzi, and L. Van Langenhove, "A textile antenna for off-body communication integrated into protective clothing for firefighters," *IEEE Trans. Antennas Propag.*, vol. 57, no. 4, pp. 919–925, April 2009.

[21] Q. Bai and R. Langley, "Crumpling of PIFA textile antenna," *IEEE Trans. Antennas Propag.*, vol. 60, no. 1, pp. 63–70, January 2012.

[22] F. Boeykens, L. Vallozzi, and H. Rogier, "Cylindrical bending of deformable textile rectangular patch antennas," *International Journal of Antennas and Propagation*, vol. 420, no. 11, pp. 1–11, Article ID 170, doi:10.1155/2012/170 420, 2012.

[23] P. Sumant, H. Wu, A. Cangellaris, and N. Aluru, "Reduced-order models of finite element approximations of electromagnetic devices exhibiting statistical variability," *IEEE Trans. Antennas Propag.*, vol. 60, no. 1, pp. 301–309, January 2012.

[24] M. Rossi, S. Agneessens, H. Rogier, and D. Vande Ginste, "Stochastic analysis of the impact of substrate compression on the performance of textile antennas," *IEEE Trans. Antennas Propag.*, vol. 64, no. 6, pp. 2507–2512, 2016.

[25] C. Salis and T. Zygiridis, "Dimensionality reduction of the polynomial chaos technique based on the method of moments," *IEEE Antennas Wireless Prop. Lett.*, vol. 17, no. 12, pp. 2349–2353, 2018.

[26] G. J. K. Tomy and K. J. Vinoy, "A fast polynomial chaos expansion for uncertainty quantification in stochastic electromagnetic problems," *IEEE Antennas Wireless Prop. Lett.*, vol. 18, no. 10, pp. 2120–2124, 2019.

[27] A. C. Yücel, H. Bagci, and E. Michielssen, "An ME-PC enhanced HDMR method for efficient statistical analysis of multiconductor transmission line networks," *IEEE Trans. Comp., Hybr., Manufac. Techn.*, vol. 5, no. 5, pp. 685–696, 2015.

[28] R. Hu, V. Monebhurrun, R. Himeno, H. Yokota, and F. Costen, "An adaptive least angle regression method for uncertainty quantification in FDTD computation," *IEEE Trans. Antennas Propag.*, vol. 66, no. 12, pp. 7188–7197, 2018.

[29] J. Du and C. Roblin, "Stochastic surrogate models of deformable antennas based on vector spherical harmonics and polynomial chaos expansions: Application to textile antennas," *IEEE Trans. Antennas Propag.*, vol. 66, no. 7, pp. 3610–3622, 2018.

[30] H. Acikgoz and R. Mittra, "Stochastic polynomial chaos expansion analysis of a split-ring resonator at terahertz frequencies," *IEEE Trans. Antennas Propag.*, vol. 66, no. 4, pp. 2131–2134, 2018.

[31] J. Du and C. Roblin, "Statistical modeling of disturbed antennas based on the polynomial chaos expansion," *IEEE Antennas Wireless Prop. Lett.*, vol. 16, pp. 1843–1846, 2017.

[32] M. Rossi, A. Dierck, H. Rogier, and D. Vande Ginste, "A stochastic framework for the variability analysis of textile antennas," *IEEE Trans. Antennas Propag.*, vol. 62, no. 12, pp. 6510–6514, 2014.

[33] E. W. Stacy and G. A. Mihram, "Parameter estimation for a generalized gamma distribution," *Technometrics*, vol. 7, no. 3, pp. 349–358, 1965.

[34] O. Gomes, C. Combes, and A. Dussauchoy, "Parameter estimation of the generalized gamma distribution," *Math. Comput. Simul.*, vol. 79, no. 4, pp. 955–963, 2008.

[35] R. J. Rossi, *Mathematical Statistics: An Introduction to Likelihood Based Inference*. New York: John Wiley & Sons., 2018.

[36] X. Shang and H. K. T. Ng, "On parameter estimation for the generalized gamma distribution based on left-truncated and right-censored data," *Comput. Math. Methods*, vol. 3, no. 1, p. e1091, 2021.

[37] K. O. Bowman and L. R. Shenton, *Estimation: Method of Moments*. John Wiley & Sons, Ltd, 2006. [Online]. Available: https://onlinelibrary.wiley.com/doi/abs/10.1002/0471667196.ess1618.pub2

[38] G. Golub and J. Welsch, "Calculation of Gauss quadrature rules," *Math. Comput.*, vol. 23, no. 106, pp. 221–230, Apr 1969.

[39] C. C. Gordon, C. L. Blackwell, B. Bradtmiller, J. Parham, P. Barrientos, P. P. Paquette, B. C. BD, J. Carson, J. C. Venezia, B. Rockwell, M. Mucher, and S. Kristensen. (2014, Dec.) 2012 anthropometric survey of U.S. Army personnel: methods and summary statistics, technical report natick/tr-15/007, U.S. Army Natick soldier research, development and engineering center, Natick, Massachusetts. [Online]. Available: http://www.dtic.mil/dtic/tr/fulltext/u2/a611869.pdf

[40] Centers for Disease Control and Prevention. (2011, Sep.) National Health and Nutrition Examination Survey. [Online]. Available: http://www.cdc.gov/nchs/nhanes.htm

[41] G. Heinz, L. J. Peterson, R. W. Johnson, and C. J. Kerk, "Exploring relationships in body dimensions," *Journal of Statistics Education*, vol. 11, no. 2, 2003. [Online]. Available: https://doi.org/10.1080/10691898.2003.11910711

[42] T. W. Anderson, "On the distribution of the two-sample Cramér-von Mises criterion," *Ann. Math. Statist.*, pp. 1148–1159, 1962.

[43] *Multivariate Gamma Distributions*. John Wiley & Sons, Ltd, 2000, ch. 48, pp. 431–483. [Online]. Available: https://onlinelibrary.wiley.com/doi/abs/10.1002/0471722065.ch48

[44] D. S. Jayakumar, A. Sulthan, and W. Samuel, "The bivariate extension of Amoroso distribution," *Indones. J. Sci. Technol.*, vol. 4, no. 2, pp. 261–283, Jul. 2020.

[45] D. Joseph, "Multivariate extended gamma distribution," *Axioms*, vol. 6, pp. 1–12, Art. nr. 11, Apr. 2017.